Analysis of Seasonal and Interannual Variations in the Positions of Permanent GPS Tracking Stations

Dr. Xiaoli L. DING, D. W. ZHENG, Y. Q. CHEN, C. HUANG and W. CHEN, China

Keywords: GPS, Station Solution, Seasonal and Interannual Signals.

ABSTRACT

Time series of daily station solutions of eight permanent GPS tracking stations located in the Pacific region are adopted to analyze the frequency features in the data. The GPS tracking stations are part of the IGS network and the daily solutions carried out by the JPL are used. The study shows that there are seasonal and interannual signals in all the three coordinate components beside the general linear trends of movement of the stations. The seasonal signals show some quasi-periodic oscillations and the strongest oscillations appear in the height component. The seasonal oscillations in the height component amount to about 3-6 mm. The strongest interannual signals also appear in the height component that are up to about 12 mm.

CONTACT

Dr. Xiaoli L. Ding
Department of Land Surveying and Geo-Informatics
The Hong Kong Polytechnic University
Hung Hom, Kowloon, Hong Kong
CHINA
Tel. + 852 2766 5965
Fax + 852 2330 2994
E-mail: lsxlding@polyu.edu.hk
Web site: http://www.polyu.edu.hk

Analysis of Seasonal and Interannual Variations in the Positions of Permanent GPS Tracking Stations

Dr. Xiaoli L. DING, D. W. ZHENG, Y. Q. CHEN, C. HUANG and W. CHEN, China

1. INTRODUCTION

GPS has over the past decade or so rapidly become one of the most important observational tool for study the rotation of the Earth, plate motions, crustal deformations, and seismic activities [e.g., Lindqwister et al., 1991; Springer et al., 1994; Zheng et al., 1995; Zumberge et al., 1997; Dong et al., 1998; Altiner, 2001; Dietrich et al., 2001; Liu et al., 2001; Miller et al., 2001]. The IGS (International GPS Service) represents a major effort of the worldwide scientific community in promoting international standards for GPS data acquisition and analysis, and in deploying and operating a common, comprehensive global tracking system. The IGS has been successfully providing GPS orbits, tracking data, and other high-quality GPS data and data products on line in near real time to meet the objectives of a wide range of scientific and engineering applications and studies. The IGS network now has more than 250 permanent GPS tracking stations. The accuracy of daily GPS solutions provided by some of the IGS Data Analysis Centers is within a few centimeters and the accuracy of weekly solutions is within about 1 cm.

When examining data from permanent GPS tracking stations, focus has mainly been on the long-term trends of station movement. We will however in this work look into the frequency features in the solutions, especially those on the seasonal to interannual time scales. A number of IGS permanent GPS stations located in the Pacific region will be used for the study. The possible impact of the detected seasonal and interannual oscillations on the estimation of linear rates of station motions will also be evaluated.

2. DATA SETS OF STATION SOLUTIONS

The daily solution time series of eight IGS permanent tracking stations located in the Pacific region (Figure 1 and Table 1) are used in the study. The daily solutions carried out by the GPS Analysis Center at the Jet Propulsion Laboratory (JPL), California Institute of Technology, are adopted. The solutions were obtained with the GIPSY software and the point positioning strategy was used (Zumberge et al., 1997). Satellite orbits were fixed to JPL precise orbits adjusted from 42 globally distributed tracking sites. For point positioning, parameters between sites are uncorrelated, so that the time series are estimated site by site. For each site, the daily solution gives the site position parameters, the stochastic zenith delay and its gradient, the white noise stochastic receiver clock parameters and the real-value carrier phase ambiguities. The JPL analysis uses an elevation cut off angle of 15 degrees, and a consistent processing strategy and software version.

It can be seen from the table and Figure 1 that stations YAR1 and PERT as well as KOKB and MKEA are relatively closer to each other. The time series of the daily solutions are plotted in Figure 2.

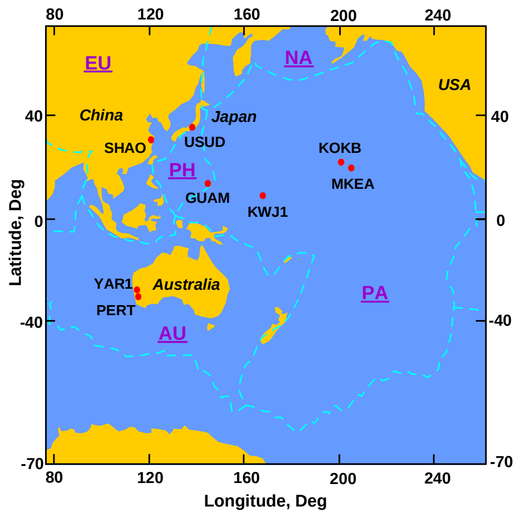

Figure 1. The GPS sites adopted for the study

Table 1. Summary of GPS data used

Code	Location	Longitude (degree)	Latitude (degree)	Time span	Number of daily solns.
YAR1	Mingenew, Australia	115.35	–29.05	5/1992-10/2000	2519
PERT	Perth, Australia	115.89	–31.80	6/1994-10/2000	1826
SHAO	Shanghai, China	121.20	31.10	1/1995-10/2000	1616
USUD	Usuda, Japan	138.36	36.13	11/1992-10/2000	2099
GUAM	Guam	144.86	13.59	1/1995-10/2000	1763
KWJ1	Marshall Island	167.73	8.72	3/1996-10/2000	1205
KOKB	Kokee Park, USA	200.34	22.13	5/1992-10/2000	2482
MKEA	Mauna Kea, USA	204.54	19.80	8/1996-10/2000	1349

3. SEASONAL AND INTERANNUAL SIGNALS

3.1 Time-Frequency Spectrum

To examine the seasonal and interannual signals in the GPS solutions, the technique of time-frequency wavelet transform is applied in this study. Given a time series *f*(*t*), its wavelet transform is defined as (Chao et al., 1995; Zheng et al., 2000).

$$W_{\psi}(f)(a,b) = \frac{1}{\sqrt{a}} \int_{-\infty}^{\infty} f(t)\psi\left(\frac{t-b}{a}\right)dt \tag{1}$$

where $\Psi(t)$ is the basic wavelet; *a* is the dilation/compression scale factor that determines the characteristic frequency; and *b* is the sliding factor in time domain. We will apply in this paper the normalized Morlet wavelet (Morlet et al., 1982) and take the real part of the wavelet transform to characterize the spectrum analysis of a real series. The phase and amplitude information of the signal in the data series can be described with the time-varying equal intensity color spectrum of wavelet transform. The main feature of wavelet transform is that the process of changes in the signals in a data series can be simultaneously displayed in the time-frequency domain (or referred to as *a-b* space), and the spectral distributions of signals of different frequencies can be visualized over the same time span.

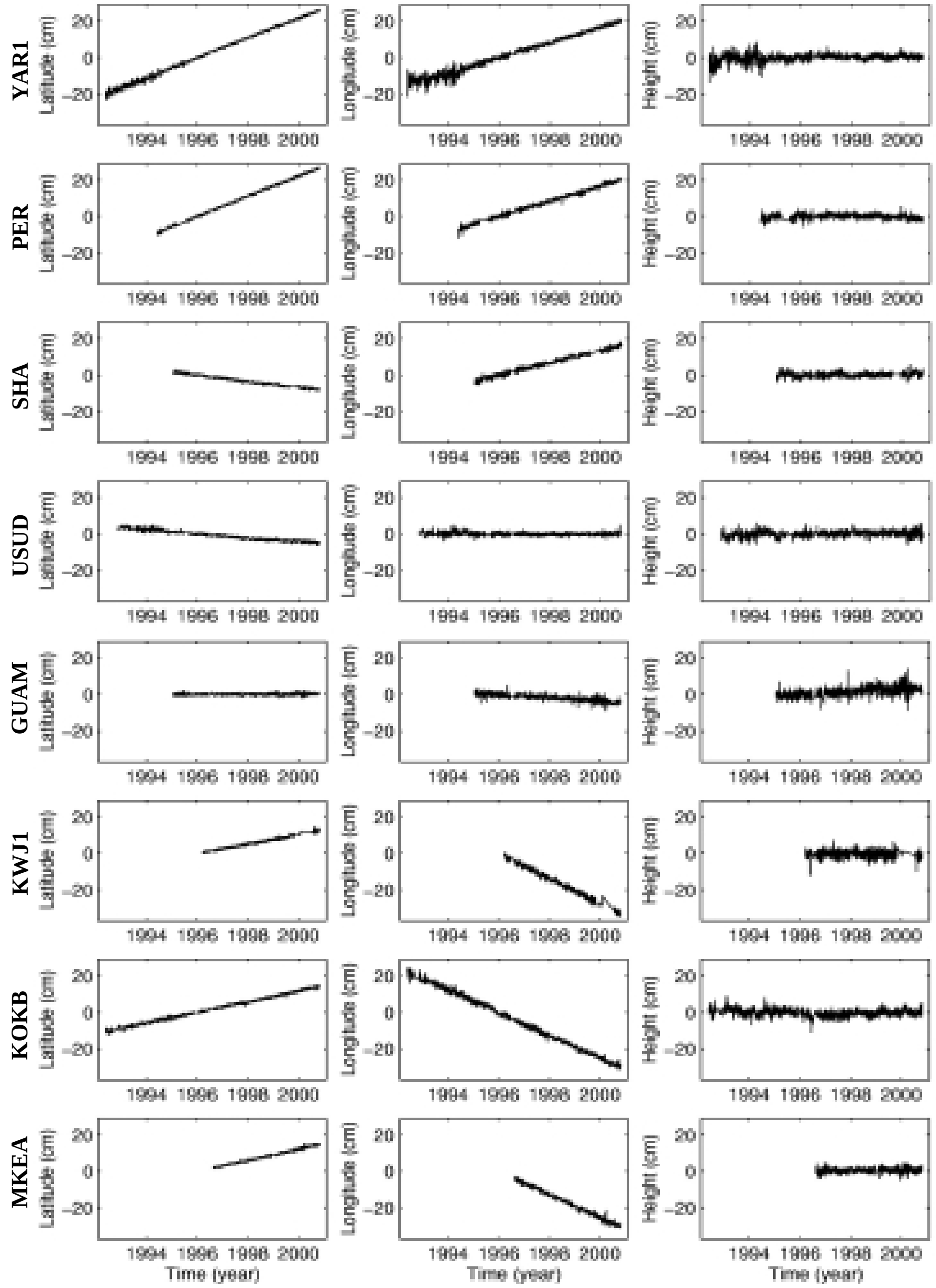

Figure 2. Time series of daily solutions of the GPS stations.

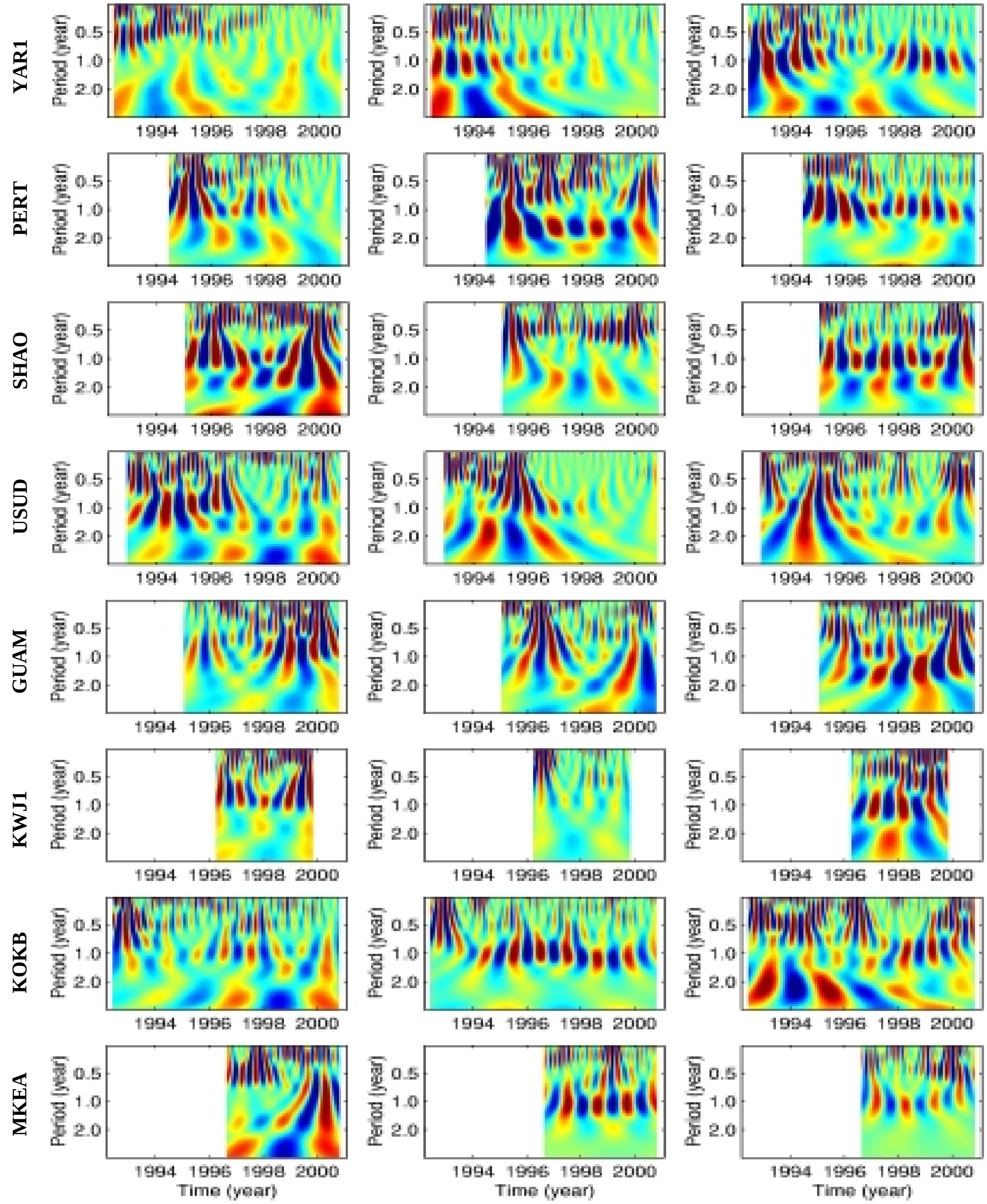

Figure 3. The wavelet spectra of the 10-day mean solutions for eight GPS

Before the wavelet spectrum is computed, 10-day mean series were first obtained from the daily solutions. For data gaps of 1-6 months in the daily solutions, the method of cubic spline interpolation was applied to derive the 10-day data in the gaps from the monthly mean series of the daily solutions. The time-frequency spectra of wavelet transform of the three coordinate components were estimated based on the 10-day mean series. The results are plotted in Figure 3. The wavelet spectra of the latitude, longitude and height components of each station are given in the plots on the left, the middle and the right of each row in the figure. For data gaps of six months or longer, such as that of post-November 1999 data for station KWJ1, the spectral estimations were not calculated.

Seasonal, semiannual and annual signals of different amplitudes can be detected in all three coordinate components of the coordinate series as seen in Figure 3. The strength and frequency of the signals vary with both time and stations, and are also different between the three coordinate components. The height component demonstrated the strongest and most stable signals for all the stations. In addition, spectral signals of lower frequency bands can also be observed from the wavelet spectra.

3.2 Seasonal Signals

The method of least squares is used to determine the magnitudes and phases of the seasonal signals detected in the wavelet spectra. Using the time series of daily solutions shown in Figure 2, the amplitudes and phases of the annual and semiannual signals, as well as a constant and the linear rate of change are simultaneously estimated for each of the time series with the least squares method of Householder Transform (Feng et al., 1978). The estimation is based on the following equation,

$$S_t = a + bt + \sum_{k=1}^{2} c_k \sin(2\pi t / P_k + \varphi_k) + \varepsilon_t \qquad (2)$$

where, P_k, c_k and φ_k are the periods, amplitudes and phases of the annual and semiannual signals, respectively, while a and b are the constant and the linear rate. The estimated results are listed in Tables 2, 3 and 4. The estimated phases are referred to the epoch of January 1997.

It can be seen from the estimated results given in Tables 2 and 3 that the amplitudes of the annual and semiannual signals for the latitude and longitude components are relatively small, and that they are up to about 1 mm and 3 mm, respectively. Comparatively, the long-term trends of movements are more dominant in the horizontal directions (see the left and the

Table 2. The estimated annual and semiannual signals in the latitude component. The phases are referred to January 1997

Station Code	Annual		Semiannual	
	Amplitude(mm)	Phase(yr.)	Amplitude(cm)	Phase(yr.)
YAR1	0.70±0.12	0.14±0.03	0.49±0.12	0.15±0.02
PERT	0.61±0.11	0.32±0.03	0.64±0.11	0.19±0.01
SHAO	1.10±0.14	0.11±0.02	0.46±0.14	0.03±0.02
USUD	0.77±0.15	-0.03±0.03	1.03±0.15	0.05±0.01
GUAM	0.45±0.14	0.21±0.05	0.78±0.14	0.13±0.01
KWJ1	0.55±0.17	0.29±0.05	0.47±0.16	-0.10±0.03
KOKB	0.67±0.12	-0.22±0.03	0.30±0.12	-0.06±0.01
MKEA	0.55±0.13	-0.02±0.04	0.98±0.13	-0.06±0.01

Table 3. The estimated annual and semiannual signals in the longitude component. The phases are referred to January 1997

Station Code	Annual		Semiannual	
	Amplitude(mm)	Phase(yr.)	Amplitude(cm)	Phase(yr.)
YAR1	1.05±0.23	-0.38±0.04	0.56±0.23	0.08±0.03
PERT	0.73±0.19	0.12±0.04	0.97±0.19	-0.15±0.02
SHAO	1.10±0.22	-0.41±0.03	2.09±0.21	-0.23±0.01
USUD	0.95±0.21	0.33±0.04	0.27±0.21	0.11±0.06
GUAM	1.50±0.29	0.35±0.03	0.80±0.28	0.23±0.03
KWJ1	1.34±0.31	0.07±0.04	0.97±0.31	-0.20±0.03
KOKB	2.72±0.22	-0.34±0.01	0.45±0.22	-0.10±0.04
MKEA	2.34±0.24	-0.34±0.02	0.42±0.23	-0.16±0.04

Table 4. The estimated annual and semiannual signals in the height component. The phases are referred to January 1997

Station code	Annual		Semiannual	
	Amplitude(mm)	Phase(yr.)	Amplitude(cm)	Phase(yr.)
YAR1	5.52±0.34	0.18±0.01	0.76±0.33	-0.18±0.01
PERT	5.13±0.36	0.22±0.01	0.47±0.35	0.06±0.05
SHAO	5.63±0.33	-0.24±0.01	2.09±0.33	0.01±0.01
USUD	2.40±0.37	-0.32±0.02	2.02±0.37	0.10±0.01
GUAM	3.35±0.53	0.35±0.02	3.45±0.52	0.11±0.01
KWJ1	3.50±0.62	0.06±0.03	2.05±0.62	-0.06±0.02
KOKB	3.79±0.41	-0.05±0.02	3.75±0.41	-0.03±0.01
MKEA	3.80±0.40	0.01±0.02	2.02±0.41	-0.19±0.02

middle plots in Figure 2). The seasonal signals in the longitude component are generally stronger than those in the latitude component. It is also interesting to note that the estimated amplitudes and phases of the annual and semiannual signals of KOKB and MKEA as listed in Table 3 are quite consistent with each other.

Both the annual and semiannual signals in the height components (Table 4) are much stronger than the corresponding ones in the latitude and longitude components. The estimated amplitudes of the signals in the height component range from 2.4 mm to 5.6 mm for the annual signals and from 0.5 mm to 3.8 mm for the semiannual signals. It is interesting to note that the estimated amplitudes and phases of the annual signals for stations that are close to each other, i.e., YAR1 and PERT, and KOKB and MKEA are quite consistent with each other. Therefore the reasons that cause the annual variations may be the same for the stations.

3.3 Interannual Signals

The least squares residuals from the daily station solutions for each of the three coordinate components are calculated using equation (2). The monthly mean residuals are then obtained by simply averaging the daily residuals of each month, and are plotted in Figure 4 as the thin lines. It can be seen from the monthly mean residual series that besides some slow fluctuations in the data, there are signals that are down to the time scales of seasonal or below. The residuals are also filtered by calculating a seven-point moving average for each of the monthly mean residual series. The results are plotted in Figure 4 as the thick lines.

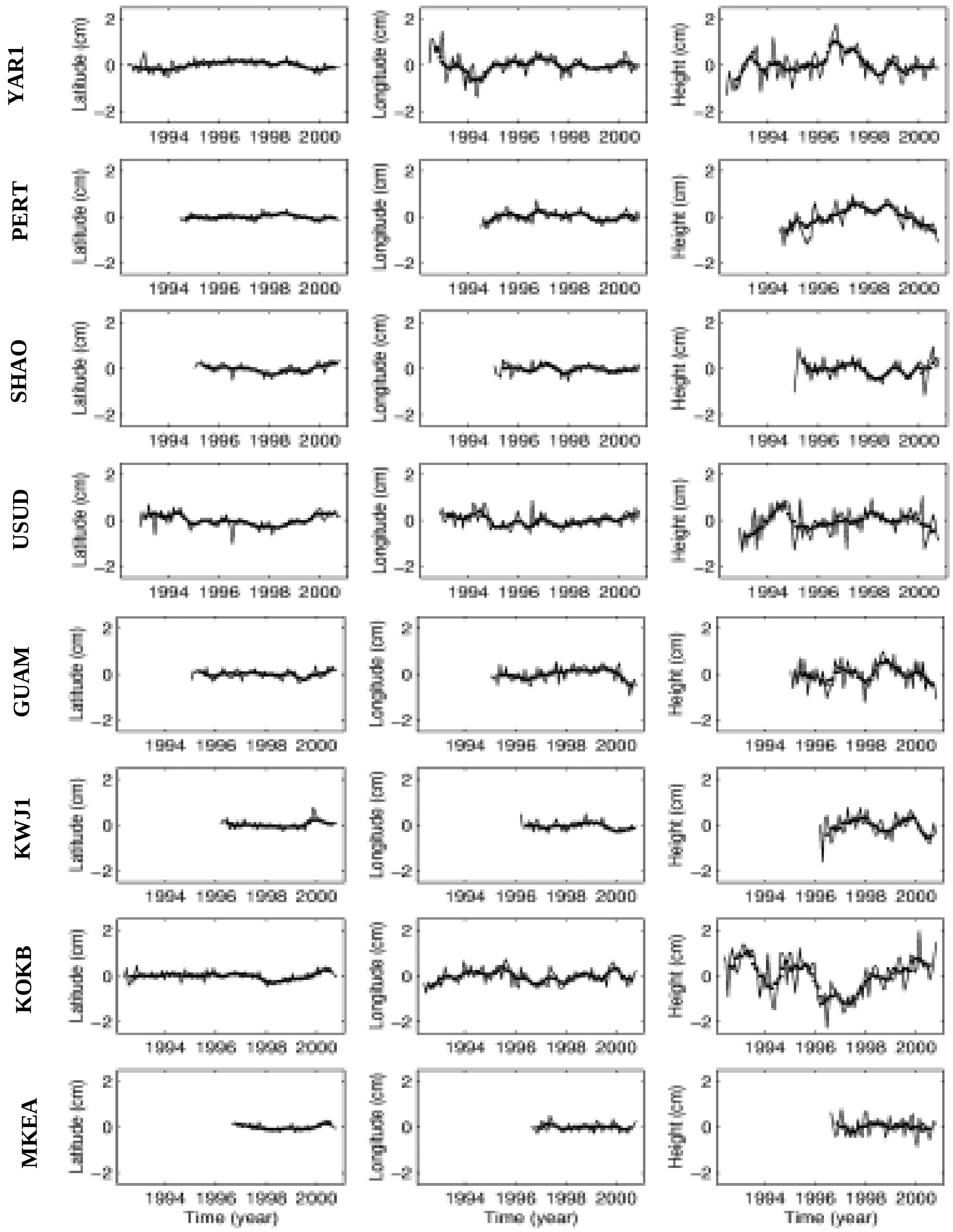

Figure 4. Monthly mean residuals (thin lines) and interannual signals (thick lines)

The filtered monthly residuals can be considered as the "interannual" signals. It can be seen from the results that there are obviously various interannual fluctuations in all the three coordinate components of the stations. The magnitudes of the signals are as high as about 3, 7 and 12 mm in the latitude, longitude and height components, respectively. The results indicate that the vertical motions of the GPS stations are accompanied by strong oscillations of fairly low frequency bands.

4. SUMMARY AND CONCLUSIONS

Daily solution time series of eight permanent GPS tracking stations distributed in the Pacific region have been analyzed to assess the frequency features in the data series. The following conclusions can be drawn from the study.

Seasonal and interannual signals in all the three coordinate components of the GPS solutions have been detected. The strengths and periods of the signals vary with time, stations and coordinate components of the stations. The signals in the latitude and longitude components are relatively weak and the long-term trends of horizontal movements of the stations are more dominant compared to the fluctuations. The seasonal signals in the height components of the stations are quite strong with the maximum amplitudes of the annual and semiannual variations amounting to 5.6 and 3.8 mm, respectively. The amplitudes and phases of the annual signals of the height components are quite consistent with each other for stations that are close. Therefore, the annual variations in the height components may have been caused by the same factors.

The frequency structures of the time series of the eight permanent GPS tracking stations in the pacific region have been analyzed. The results are however preliminary and it is still necessary to analyze the solutions further, especially with the increase of the lengths of the data series. Besides, the reasons that caused the seasonal and interannual variations in the data series still need investigated.

ACKNOWLEDGEMENTS

The authors are grateful to Dr. D.N. Dong and Dr. J.F. Zumberge of JPL for their kind assistance, useful discussions and suggestions. This work was partly supported by the Research Grants Council of the Hong Kong Special Administrative Region (PolyU 5067/00E), the National Key Project in China, the National Natural Science Foundation of China and the Chinese Academy of Sciences (Project numbers: 970231003, 19833030 and KJ951-1-304).

REFERENCES

Altiner, Y. (2001), The contribution of GPS data to the detection of the Earth's crust deformations illustrated by GPS campaigns in the Adria region, *Geophys J. Int.,* 145 (2): 550-559.

Chao, B.F. and Naito, I. (1995) Wavelet analysis provide a new tool for studying Earth Rotation, *EOS*, 76, 161-165.

Dietrich, R., Dach, R., Engelhardt, G., Ihde, J., Korth, W., Kutterer, H.J., Lindner, K., Mayer, M., Menge, F., Miller, H., Muller, C., Niemeier, W., Perlt, J., Pohl, M., Salbach, H., Schenke, H.W., Schone, T., Seeber, G., Veit, A. and Volksen, C. (2001), ITRF

coordinates and plate velocities from repeated GPS campaigns in Antarctica - an analysis based on different individual solutions, *J. Geody.*, 74 (11-12): 756-766.
Dong, D., Herring, T.A. and King, R.W. (1998), Estimating regional deformation from a combination of space and terrestrial geodetic data, *J. Geod.*, 72 (4): 200-214.
Feng, K., Zhang, J., Zhang, Y., Yang, Z. and Chao, W. (1978) *Numerical Calculation Method*, National Defense Industry Press, Beijing, 311p.
Lindqwister, U.J., Zumberge, J.F., Webb, F.H. and Blewitt, G. (1991), Few millimeter precision for base-lines in the California permanent GPS geodetic array, *Geophys. Res. Lett.*, 18 (6): 1135-1138.
Liu, J.Y., Chen, Y.I., Chuo, Y.J. and Tsai, H.F. (2001), Variations of ionospheric total electron content during the Chi-Chi earthquake, *Geophys Res. Lett.*, 28 (7): 1383-1386.
Miller, M.M., Johnson, D.J., Rubin, C.M., Dragert, H., Wang, K., Qamar, A. and Goldfinger, C. (2001) GPS-determination of along-strike variation in Cascadia margin kinematics: Implications for relative plate motion, subduction zone coupling, and permanent deformation, *Tectonics,* 20 (2): 161-176.
Morlet, J., Arehs, G., Fourgeau, I. and Giard, D. (1982), Wave propagation and sampling theory, *Geophysics*, 47, 203-221.
Springer, T.A., Ambrosius, B.A.C., Noomen, R. and Herzberger, K. (1994), Results of the wegener/GPS-92 Campaign, *Geophys. Res. Lett.*, 21(16): 1711-1714.
Zheng, D.W., Xie, B.Q. (1995) High-frequency resolution of Earth orientation parameter measured by GPS, *Chinese Science Bull*., 40 (12): 1012-1016.
Zumberge, J.F., Heflin, M.B., Jefferson, D.C., Watkins, M.M. and Webb, F.H. (1997), Precise point positioning for the efficient and robust analysis of GPS data from large networks, *J. Geophys. Res.-Solid Earth,* 102 (B3): 5005-5017. Zheng, D.W., Chao, B.F., Zhou, Y.H. and Yu, N.H. (1999) Improvement of edge effect of the wavelet time-frequency spectrum: application to the length of day series, *J Geod*, 74(2), 249-254.